actuators

MDPI

Article

L1 Adaptive Fault-Tolerant Control for Nonlinear Systems Subject to Input Constraint and Multiple Faults

Yan Zhou [1,*], Huiying Liu [2] and Huijuan Guo [3]

[1] School of Electronic and Electrical Engineering, Zhaoqing University, Zhaoqing 526061, China
[2] School of Automation, Northwestern Polytechnical University, Xi'an 710129, China; lhy2005@nwpu.edu.cn
[3] School of Information Engineering, Suqian University, Suqian 223800, China; 17177@squ.edu.cn
* Correspondence: zhouyan@zqu.edu.cn

Abstract: This paper investigates an L1 adaptive fault-tolerant control scheme for nonlinear systems with input constraint, external disturbances, and multiple faults, which include actuator faults and sensor faults. Faults and input constraint are important factors that affect the stability and performance of a control system. Actuators and sensors are the most vulnerable components, with the former receiving more attention in comparison. In this paper, sensor faults are first transformed into pseudo-actuator faults through the augmented matrix approach, which facilitates their handling together with actuator faults. Saturation constraints on the control signal are not conducive to the design of the controller. The conversion of an input-saturated function to a time-varying linear system is completed based on function approximation and Lagrange's mean value theorem. Moreover, a nonlinear system with unknown input gain and uncertainties is constructed using these methods. Next, an L1 adaptive fault-tolerant controller is designed to cope with uncertainties, including system uncertainties, external disturbances, faults, and approximation errors. In the L1 adaptive controller, the online estimation of the time-varying parameters allows for updating of the system state, while the combination of the two is transmitted to the control law such that it can compensate for the effects of the uncertainties. The stability and performance boundaries are further derived using the Lyapunov theory and the L1 reference system. Finally, simulations are carried out to demonstrate the effectiveness of the proposed controller.

Keywords: fault-tolerant control; L1 adaptive control; actuator fault; input constraint; sensor fault

check for updates

Citation: Zhou, Y.; Liu, H.; Guo, H. L1 Adaptive Fault-Tolerant Control for Nonlinear Systems Subject to Input Constraint and Multiple Faults. *Actuators* **2024**, *13*, 258. https://doi.org/10.3390/act13070258

Academic Editors: Guangtao Ran, Yanning Guo and Chuan-jiang Li

Received: 29 May 2024
Revised: 6 July 2024
Accepted: 8 July 2024
Published: 9 July 2024

Copyright: © 2024 by the authors. Licensee MDPI, Basel, Switzerland. This article is an open access article distributed under the terms and conditions of the Creative Commons Attribution (CC BY) license (https://creativecommons.org/licenses/by/4.0/).

1. Introduction

Actuators and sensors are the essential bridge to understanding how a control system works and are also the most fault-prone components. Actuators implement control instructions, and their faults may have serious impacts on the system, such as control deviation, disturbance, or even system destabilization. Sensors are used to measure parameters that are necessary for control systems. Errors in measurement data may result in poor control. In recent years, many control methods have been developed to overcome single faults, such as actuator faults or sensor faults [1–6]. However, the actual control system may have actuator faults and sensor faults concurrently; therefore, a fault-tolerant control system that takes into account actuator and sensor faults is preferable.

Fault-tolerant control based on fault detection, diagnosis, and isolation (FDI) techniques is one of the most important branches of control system design, especially observer-based fault detection and isolation, such as optimal observer [7], Kalman filter [8,9], and adaptive observer [10]. In [11], a distributed fault detection observer and an estimation observer based on sliding mode technology were designed. Based on the concept of switching, adaptive fault-tolerant consensus control with a hierarchical structure has been realized to compensate for system nonlinearities, uncertainties, and actuator faults [12]. In [13], the amplitude and rate faults in actuators were investigated using adaptive observers.

Observer-based FDI techniques are widely used not only for actuator faults but also for sensor faults [1,14–18]. In addition, fault-tolerant control strategies based on fault values from fault estimators are also an effective approach. For an aircraft attitude control system with actuator faults and sensor faults, a fault-tolerant controller based on estimates of actuator faults and sensor faults from two extended state observers has been discussed in [19]. A sliding mode fault-tolerant controller with dynamic event-triggered fault estimation for networked control systems was implemented in [20]. Moreover, in [21], a fault-tolerant controller for interval type-2 polynomial fuzzy systems subject to sensor faults and actuator faults was presented through fault estimation. Throughout most of the current research results, fault-tolerant controllers mainly rely on fault detection or estimation, which carry certain limitations and involve complicated algorithms. However, a new fault-tolerant control scheme that does not require fault information has been developed over the past few years.

Input saturation is a kind of nonlinear constraint that actually exists in actuators, which may affect the stability and reliability of the control system. The problem of input constraint has always been a hot topic, and various control methods have been explored, such as constructing auxiliary systems [22–24] and directly designing anti-saturation controllers [25,26]. It is also recommended to build a variety of valid controllers based on the practice of approximating the saturation function with some nonlinear smooth functions, such as the hyperbolic tangent function [27,28] and the sigmoid function [29]. In real systems, input constraint, multiple faults, and external disturbances often occur, even simultaneously. The interaction of these factors aggravates the system uncertainties and makes the detection or estimation of faults more difficult; thus, the performance of the fault-tolerant controller is likely to be degraded. Therefore, the successful design of an effective fault-tolerant controller under the influence of system uncertainties, faults, input constraint, and external disturbances remains a challenge.

A novel fault-tolerant control method based on adaptive online estimation has been developed [30–34]. Viewing faults, input constraint, and external disturbances as a lumped uncertainty, this method does not need to detect or estimate faults and can effectively simplify the structure of the fault-tolerant controller. Motivated by the above-mentioned analyses, in this paper, a nonlinear system model with input constraint and external disturbances is developed, while considering both actuator and sensor faults. Through a series of transformations and reorganizations, system uncertainties, multiple faults, input constraint, and external disturbances contained in the nonlinear system are eventually constructed as unknown input gains and a lumped uncertainty. To compensate for the effects of these uncertainties, an L1 adaptive fault-tolerant controller is studied, including state predictor, adaptive law, and control law components. The L1 adaptive algorithm is a variant of the model reference adaptive control (MRAC) scheme with fast adaptation ability and excellent robustness, which is widely used in various control systems [35–37]. The state predictor is equivalent to a reference model to estimate the system state. The adaptive law updates each adaptive parameter and passes estimations of adaptive parameters to the state predictor and the control law. The control law with low-pass filters is designed to counteract the effects of uncertainties and reduce the high-frequency oscillations associated with high adaptive gains. In comparison with the existing research results, the main contributions of this paper are summarized as follows:

(1) Unlike most previous research, which addressed only one or a few scenarios, the fault-tolerant control discussed in this paper covers actuator faults, sensor faults, input constraint, and external disturbances, which are frequently experienced in control systems.

(2) In this paper, multiple faults, approximation errors and external disturbances are converted into a lumped uncertainty and estimated using adaptive laws in the L1 adaptive controller. In contrast to the methods in [19,21], the L1 adaptive controller does not require the design of additional fault observers or estimators, and

the control algorithm is more concise. Moreover, a more detailed description of the L1 adaptive controller's stability and dynamic performance is provided.

(3) Compared with the nonlinear function approximation of input constraint in [27–29], this paper further transforms the input constraint into a time-varying system with unknown parameters and disturbances, which is more conducive to the design of fault-tolerant controllers.

The remainder of this paper is organized as follows: The problem formulation is shown in Section 2. The design of the L1 adaptive fault-tolerant controller is described in Section 3. In Section 4, the performance analysis of the fault-tolerant controller is presented. In Section 5, some simulation examples are provided to demonstrate the effectiveness of the proposed controller. Finally, our conclusions are drawn in Section 6.

2. Problem Formulation

Consider the following nonlinear system with input constraint, faults, and external disturbances:

$$\begin{cases} \dot{x}(t) = Ax(t) + B(\omega u(v(t)) + \overline{u}(t)) + f(x,t) + d(t) \\ y(t) = Cx(t) + Gf_s(t) \end{cases} \tag{1}$$

where $x(t) \in R^n$ and $y(t) \in R^p$ are state variables and measurement outputs; $u(v(t)) \in R^m$ and $v(t)$ are input signals with saturated nonlinearity and actual control inputs; $f(x,t)$ is an unknown smooth nonlinear function; $d(t)$ denotes the external disturbances; and $\overline{u}(t)$ and $\omega = diag(\omega_1, \omega_2, \ldots, \omega_m)$ represent the additive and multiplicative actuator faults, respectively. Additive and multiplicative faults are the most common types of actuator faults and can indicate most of the actual actuator faults, such as loss of effectiveness, stuck, and float. $f_s(t) \in R^q$ denotes the unknown sensor faults, and only bias sensor faults are considered in this paper, including constant deviation faults and drift faults. $A \in R^{n\times n}$, $B \in R^{n\times m}$, $C \in R^{p\times n}$, and $G \in R^{p\times q}$ are known constant matrices.

The saturation function $u(v(t))$ is described as follows:

$$u(v(t)) = sat(v(t)) = \begin{cases} -u_m, v \le -u_m \\ v, -u_m < v < u_m \\ u_m, v \ge u_m \end{cases} \tag{2}$$

where u_m is the known boundary of the saturation function $u(v(t))$, which is, the physical limit of the actuator's output.

Following convention, some basic definitions and assumptions are recalled or introduced for the purpose of the latter presentation [38–40].

Definition 1. *For a signal $r(t), t \ge 0, r \in R^m$, its ∞-norm and L_∞-norm are defined as follows:* $\|r\|_\infty = \max\limits_{1\le i\le m} |r_i|$, $\|r_t\|_{L_\infty} = \max\limits_{i=1,\ldots,m} \left(\sup\limits_{0\le\tau\le t} |r_i(\tau)| \right)$.

Definition 2. *For a given m-input and n-output linear time-invariant system $H(s)$, its L_1-norm is defined as follows:* $\|H(s)\|_{L_1} = \max\limits_{i=1,\ldots,n} \left(\sum\limits_{j=1}^{m} \|H_{ij}(s)\|_{L_1} \right)$.

Definition 3. *Consider a convex compact set with a smooth boundary provided by $\Omega_c = \{\theta \in R^n | f(\theta) \le c\}, 0 \le c \le 1$, where $f : R^n \to R$ is the smooth convex function as follows:*

$$f(\theta) = \frac{(\varepsilon_\theta + 1)\theta^T\theta - \theta_{\max}^2}{\varepsilon_\theta \theta_{\max}^2},$$

with θ_{max} is the norm bound of the vector θ, and $\varepsilon_\theta > 0$ is the projection perturbation bound selected according to the accuracy requirements of the parameters. The projection operator is defined as follows:

$$proj(\theta, y) = \begin{cases} y, & f(\theta) < 0 \\ y, & f(\theta) \geq 0 \text{ and } \nabla f^T y \leq 0 \\ y - \frac{\nabla f}{\|\nabla f\|} \left\langle \frac{\nabla f}{\|\nabla f\|}, y \right\rangle f(\theta), & f(\theta) \geq 0 \text{ and } \nabla f^T y > 0 \end{cases}$$

where $\nabla f(\cdot)$ is the gradient of $f(\cdot)$, $\frac{\nabla f}{\|\nabla f\|}$ denotes the unitization of the vector $\nabla f(\cdot)$, and $\left\langle \frac{\nabla f}{\|\nabla f\|}, y \right\rangle$ is the inner product of two vectors $\frac{\nabla f}{\|\nabla f\|}$ and y.

Assumption 1. *Let $\omega \in \Omega \triangleq [\omega_l, \omega_h]$, where ω_l and ω_h are the known boundaries of the multiplicative actuator fault ω.*

Assumption 2. *There exists $B_i > 0 (i = 1, \ldots, 4)$ such that*

$$\|f(0,t)\|_\infty \leq B_1, \|f_s(t)\|_\infty \leq B_2, \|d(t)\|_\infty \leq B_3, \|\overline{u}(t)\|_\infty \leq B_4.$$

Remark 1. *Assumptions 1 and 2 indicate that faults, system uncertainties, and external disturbances are all bounded. In the actual control system, it is possible for these assumptions to be satisfied. Taking the attitude control system of an aircraft as an example, the system uncertainty $f(x,t)$ is a nonlinear function related to the aerodynamic parameters. When the aircraft is flying normally within the flight envelope, all parameters within the control system are bounded; therefore, the system uncertainty is also bounded, as are sensor faults and external disturbances. Whether the faults are multiplicative or additive, time-varying or constant, the actuator outputs are subject to physical constraints due to the presence of input saturation. Therefore, the actuator fault factors ω and $\overline{u}(t)$ are both bounded.*

Next, the equivalent transformation of sensor faults is realized using low-pass filters and expansion of state variables. The following low-pass filter is considered:

$$\dot{z}(t) = A_l z(t) + B_l y(t) \tag{3}$$

where $z(t) \in R^k$ represents the state variables of the filters. $A_l \in R^{k \times k}, B_l \in R^{k \times p}$ are two matrices to be designed.

Substituting the output equation of (1) into (3), leads to the following expression:

$$\dot{z}(t) = A_l z(t) + B_l C x(t) + B_l G f_s(t) \tag{4}$$

Combining Equations (1) and (4), the following expression is obtained:

$$\begin{aligned} \begin{bmatrix} \dot{x}(t) \\ \dot{z}(t) \end{bmatrix} &= \begin{bmatrix} A & 0 \\ B_l C & A_l \end{bmatrix} \begin{bmatrix} x(t) \\ z(t) \end{bmatrix} + \begin{bmatrix} B \\ 0 \end{bmatrix} (\omega u(v(t)) + \overline{u}(t)) + \begin{bmatrix} f(x,t) \\ 0 \end{bmatrix} \\ &+ \begin{bmatrix} 0 \\ B_l G \end{bmatrix} f_s(t) + \begin{bmatrix} d(t) \\ 0 \end{bmatrix} \end{aligned} \tag{5}$$

Let

$$\begin{aligned} &\overline{x}(t) = \begin{bmatrix} x(t) \\ z(t) \end{bmatrix}, \overline{y}(t) = z(t), \overline{A} = \begin{bmatrix} A & 0 \\ B_l C & A_l \end{bmatrix}, \overline{B} = \begin{bmatrix} B \\ 0 \end{bmatrix}, \\ &\overline{C} = \begin{bmatrix} 0 & I \end{bmatrix}, \overline{f}(\overline{x}, t) = \begin{bmatrix} f(x,t) \\ 0 \end{bmatrix}, \overline{G}(t) = \begin{bmatrix} 0 \\ B_l G \end{bmatrix}, \overline{d}(t) = \begin{bmatrix} d(t) \\ 0 \end{bmatrix} \end{aligned}$$

Further, the following augmented system is obtained:

$$\begin{cases} \dot{\overline{x}}(t) = \overline{A}\overline{x}(t) + \overline{B}\omega u(v(t)) + \zeta_f(\overline{x}, t) \\ \overline{y}(t) = \overline{C}\overline{x}(t) \end{cases} \tag{6}$$

where $\zeta_f(\overline{x},t) = \overline{f}(\overline{x},t) + \overline{B}\overline{u}(t) + \overline{G}f_s(t) + \overline{d}(t)$ is a lumped uncertainty that includes system uncertainty $\overline{f}(x,t)$, external disturbance $\overline{d}(t)$, and faults including an additive actuator fault $\overline{B}\overline{u}(t)$ and a sensor fault $\overline{G}f_s(t)$. Based on Assumption 2, it is clear that $\zeta_f(\overline{x},t)$ is also bounded; that is, $\|\zeta_f(0,t)\|_\infty \leq B_0, \forall t \geq 0, \overline{x}(0) = \overline{x}_0$.

The sensor faults in the original system (1) are transformed into pseudo-actuator faults by introducing the low-pass filter (3). The advantage of this transformation is that the system only needs to deal with a single actuator fault, and numerous effective fault-tolerant control methods for actuator faults can be selected.

Remark 2. *The filter parameters A_l and B_l are important factors to ensure the stability of the augmented system (6), so far there is no systematic design method. A first-order low-pass filter of $\dot{z}(t) = -A_l z(t) + A_l y(t)$ was design in [1,17] to realize the equivalent transformation of sensor faults, where $-A_l$ is a Hurwitz matrix. In this paper, the filter parameter A_l is selected similarly to the work of References 1 and 17, while parameter B_l is obtained by fine-tuning to achieve better tracking performance.*

The input constraint is a common and important nonlinear saturation limitation, which should be dealt with properly in the design of the controller. Here, the following hyperbolic tangent function is constructed to approximate the saturation function (2):

$$h(v(t)) = u_m \cdot \tanh\left(\frac{v}{u_m}\right) = u_m \cdot \frac{e^{v/u_m} - e^{-v/u_m}}{e^{v/u_m} + e^{-v/u_m}} \tag{7}$$

Figure 1 shows the actual output curves of $sat(v(t))$ and $h(v(t))$. From Figure 1, it can be observed that the hyperbolic tangent function $h(v(t))$ can approximate the saturation function $sat(v(t))$ very well and eliminate its nonlinearity. We define $e_v = sat(v(t)) - h(v(t))$, where e_v is the approximation error. Considering Equations (2) and (7), the bound of e_v is derived as follows:

$$|e_v| \leq u_m(1 - \tanh(1)) \tag{8}$$

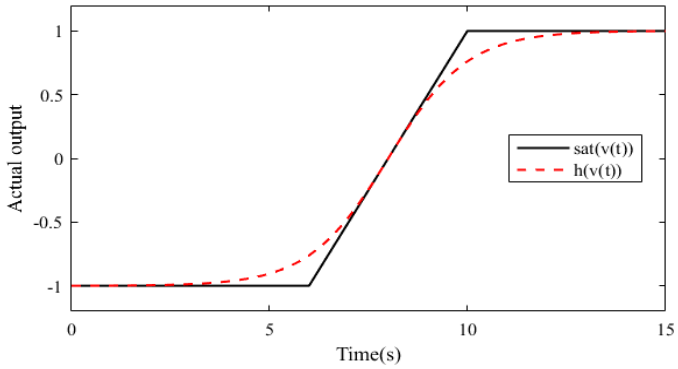

Figure 1. The output curves of saturation function and hyperbolic tangent function.

According to Lagrange's mean value theorem, let $v^*(t) = \alpha v(t), 0 < \alpha < 1$, so there must be $v^*(t)$ in the interval $(0, v)$ such that:

$$h(v(t)) = h(0) + \left.\frac{\partial h}{\partial v}\right|_{v=v^*} v(t) \tag{9}$$

It is obvious that $h(0) = 0$ based on (7). Furthermore, we define $h^* = \left.\frac{\partial h}{\partial v}\right|_{v=v^*}$; therefore, $h(v(t))$ can be rewritten as follows:

$$h(v(t)) = h^* v(t) \tag{10}$$

Further, the saturation function of $u(v(t))$ yields the following expression:

$$u(v(t)) = sat(v(t)) = h^* v(t) + e_v \tag{11}$$

Remark 3. *It can be observed in (7) that the approximation of the hyperbolic tangent function transforms the saturation function $sat(v(t))$ into a differentiable continuous function $h(v(t))$. The application of Lagrange's mean value theorem further decouples the continuous function into a time-varying linear system in (11), in order to simplify the system model in the next step.*

Substituting (11) into the state equation of (6), the following system is obtained:

$$\begin{cases} \dot{\overline{x}}(t) = \overline{A}\overline{x}(t) + \overline{B}_h \omega v(t) + \zeta_e \\ \overline{y}(t) = \overline{C}\overline{x}(t) \end{cases} \tag{12}$$

where $\overline{B}_h = \overline{B}h^*$ is an unknown bounded matrix to be designed. $\zeta_e = \overline{B}\omega e_v + \zeta_f(\overline{x}, t)$ is a lumped uncertainty, which is composed of system uncertainty, actuator faults, sensor faults, external disturbances, and approximation errors of the saturation function.

Assumption 3. *For arbitrary $\delta > 0$, there exist $d_{\zeta_{ex}}(\delta) > 0$, $d_{\zeta_{et}}(\delta) > 0$, such that for arbitrary $\|\overline{x}\|_\infty \leq \delta$, the partial derivatives of $\zeta_e(x, t)$ are piecewise-continuous and bounded,*

$$\left\| \frac{\partial \zeta_e(x,t)}{\partial x} \right\|_{L_\infty} \leq d_{\zeta_{ex}}(\delta), \left\| \frac{\partial \zeta_e(x,t)}{\partial t} \right\|_{L_\infty} \leq d_{\zeta_{et}}(\delta)$$

Remark 4. *Notice that the lumped uncertainty ζ_e is also bounded based on the boundedness of ω, e_v and ζ_f. For the convenience of the later formulation, the upper boundary of ζ_e is defined as: $\|\zeta_e\|_\infty \leq B_5$.*

Remark 5. *It is obvious in (12) that input constraint is used to reconstruct the input matrix of the system, and the additive actuator faults, external disturbances and approximation errors are organized as a lumped uncertainty. Therefore, neither faults nor disturbances can be estimated separately in this paper.*

Next, a linear parameterization method for nonlinear systems is presented. Subject to Assumptions 1 to 3, the following lemma indicates that a nonlinear function can be transformed into a linear system with unknown parameters and disturbances.

Lemma 1 [38]**.** *If $\|x_\tau\|_{L_\infty} \leq \rho$ and $\|\dot{x}_\tau\|_{L_\infty} \leq d_x$ for $\tau \geq 0$, where $\rho > 0, d_x > 0$, then there exist $\theta(t)$ and $\sigma(t)$ such that for all $t \in [0, \tau]$*

$$\zeta_e = \theta(t)\|\overline{x}(t)\|_\infty + \sigma(t) \tag{13}$$

where $\|\theta(t)\|_\infty \leq \theta_b$, $\|\dot{\theta}(t)\|_\infty \leq d_\theta$, $\|\sigma(t)\|_\infty \leq \sigma_b$, $\|\dot{\sigma}(t)\|_\infty \leq d_\sigma$.

Substituting (13) into the augmented system in (12), the following system model is obtained based on the matched uncertainties:

$$\begin{cases} \dot{\overline{x}}(t) = \overline{A}\overline{x}(t) + \overline{B}_h(\omega v(t) + \theta(t)\|\overline{x}(t)\|_\infty + \sigma(t)) \\ \overline{y}(t) = \overline{C}\overline{x}(t) \end{cases} \tag{14}$$

Thus far, the modeling process for a nonlinear system with input constraints, multiple faults, and external disturbances has been completed. The control objective of this paper is that the output signal $y(t)$ of the system can track the given input signal $r(t)$ with certain control performance.

3. The Design of the L1 Adaptive Fault-Tolerant Controller

An L1 adaptive controller consists of three components: a state predictor, an adaptive law, and a control law. The state predictor component is a dynamic system with adaptive parameters that approximate the actual system. The adaptive law component is designed to update each adaptive parameter. The control law component, based on adaptive parameters and state variables, is the output of the L1 adaptive controller. Different from the MRAC scheme, the L1 control law introduces a low-pass filter to eliminate undesirable high-frequency oscillations and ensure fast adaptation and robustness.

A. State Predictor

Consider the following state predictor:

$$\begin{cases} \dot{\hat{\overline{x}}}(t) = \overline{A}\hat{\overline{x}}(t) + \overline{B}_h(\hat{\omega}v(t) + \hat{\theta}(t)\|\overline{x}(t)\|_\infty + \hat{\sigma}(t)) \\ \hat{\overline{y}}(t) = \overline{C}\hat{\overline{x}}(t) \end{cases} \tag{15}$$

where $\hat{\omega}, \hat{\theta}$ and $\hat{\sigma}$ are estimates of the unknown parameters ω, θ and σ.

B. Adaptive Law

The adaptive laws of the unknown parameters ω, θ and σ are designed as follows:

$$\begin{cases} \dot{\hat{\omega}}(t) = \Gamma proj(\hat{\omega}(t), -\tilde{\overline{x}}(t)^T P\overline{B}_h v(t)) \\ \dot{\hat{\theta}}(t) = \Gamma proj(\hat{\theta}(t), -\tilde{\overline{x}}(t)^T P\overline{B}_h\|\tilde{\overline{x}}(t)\|_\infty) \\ \dot{\hat{\sigma}}(t) = \Gamma proj(\hat{\sigma}(t), -\tilde{\overline{x}}(t)^T P\overline{B}_h) \end{cases} \tag{16}$$

where $\tilde{\overline{x}}(t)$ is the error of the state variable; $\tilde{\overline{x}}(t) = \hat{\overline{x}}(t) - \overline{x}(t)$; Γ is a positive adaptive gain; P is a positive symmetric matrix and satisfies the algebraic Lyapunov equation $\overline{A}^T P + P\overline{A} = -Q, Q = Q^T > 0$; and $proj(\cdot)$ is the projection operator to guarantee the boundedness of these estimates, which is introduced in Definition 3.

C. Control Law

The following L1 adaptive control law is designed:

$$v(s) = -C(s)(\hat{\chi}(s) - k_g r(s)) \tag{17}$$

where $\hat{\chi}(s)$ and $r(s)$ are the Laplace transforms of $\hat{\chi}(t) = \hat{\omega}v(t) + \hat{\theta}(t)\|\overline{x}(t)\|_\infty + \hat{\sigma}(t)$ and the given reference command $r(t)$; k_g is chosen as $k_g = -(\overline{C}\overline{A}^{-1}\overline{B}_h)^{-1}$.

Remark 6. *The introduction of the low-pass filter $C(s)$ limits the effective bandwidth of the adaptive system, which means that the L1 adaptive controller compensates for the uncertainties within the effective bandwidth. Moreover, $C(s)$ must satisfy the following L1-norm condition to guarantee the stability of the closed-loop system. For a given constant ρ_0, there exists $\rho_r > \rho_{in}, \rho_{in} = \|s(sI - \overline{A})^{-1}\|_{L_1}\rho_0$, such that the L1-norm condition can be verified as follows:*

$$\|G(s)\|_{L_1} < \frac{\rho_r - \|H(s)C(s)k_g\|_{L_1}\|r\|_{L_\infty} - \rho_{in}}{L_{\rho_r}\rho_r + B_5} \tag{18}$$

where $L_\delta = \frac{\overline{\delta}(\delta)}{\delta} d_{\zeta_{ex}}(\overline{\delta}(\delta)), \overline{\delta}(\delta) = \delta + \bar{\varepsilon}$, in which $\bar{\varepsilon}$ is an arbitrary positive constant; and δ is defined in Assumption 3. $G(s) = H(s)(I - C(s)), H(s) = (sI - \overline{A})^{-1}\overline{B}_h$, B_5 is the boundedness of ζ_e in Remark 4. k_g and $r(t)$ are introduced in the control law of (17). If $\left\|\frac{\partial \zeta_e}{\partial x}\right\| \le d_{\zeta_{ex}} = L$, then

$$\lim_{\rho_r \to \infty} \frac{\rho_r - \|H(s)C(s)k_g\|_{L_1}\|r\|_{L_\infty} - \rho_{in}}{L_{\rho_r}\rho_r + B_5} = \frac{1}{L} \tag{19}$$

Therefore, the L1-norm condition of (18) can be rewritten as follows:

$$\|G(s)\|_{L_1} L < 1 \tag{20}$$

4. The Analysis of the L1 Adaptive Fault-Tolerant Controller

4.1. L1 Reference System

To verify the stability and performance boundaries of the L1 adaptive system, the following L1 reference system is introduced:

$$\begin{cases} \dot{\overline{x}}_{ref}(t) = \overline{A}\overline{x}_{ref}(t) + \overline{B}_h(\omega v_{ref}(t) + \zeta_e(\overline{x}_{ref}, t)) \\ v_{ref}(s) = \frac{C(s)}{\omega}(k_g r(s) - \lambda_{ref}(s)) \\ \overline{y}_{ref}(t) = \overline{C}\overline{x}_{ref}(t) \end{cases} \tag{21}$$

where $\lambda_{ref}(s)$ is the Laplace transform of $\zeta_e(\overline{x}_{ref}, t)$.

Obviously, the equation of state in (21) can easily be rewritten as follows:

$$\overline{x}_{ref}(s) = G(s)\lambda_{ref}(s) + H(s)C(s)k_g r(s) + \overline{x}_{ref0}(s) \tag{22}$$

where $G(s)$ and $H(s)$ have been introduced in (18), and $\overline{x}_{ref0}(s) = (sI - \overline{A})^{-1}\overline{x}_{ref}(0)$.

Next, in order to verify the stability of the L1 reference system (21), the following lemma is first introduced:

Lemma 2 [39]**.** *For a stable system $H(s)$ with input signal $r(t)$ and output signal $x(t)$, there exists $\forall t > 0$; the following inequality holds:*

$$\|x_t\|_{L_\infty} \leq \|H(s)\|_{L_1} \|r_t\|_{L_\infty} \tag{23}$$

The following lemma verifies the stability of the L1 reference system (21):

Lemma 3. *For the L1 reference system (21) subject to the L1-norm condition (20), if $\|\overline{x}(0)\|_\infty \leq \rho_0$, then*

$$\|\overline{x}_{ref}\|_{L_\infty} < \rho_r \tag{24}$$

$$\|v_{ref}\|_{L_\infty} < \rho_{vr} \tag{25}$$

where ρ_0 and ρ_r are introduction in L1-norm condition (18),

$$\rho_{vr} = \left\| \frac{C(s)}{\omega} \right\|_{L_1} \left(|k_g| \|r\|_{L_\infty} + L_{\rho_r}\rho_r + B_1 \right) \tag{26}$$

Proof of Lemma 3. Based on Lemma 2, it can be observed that (22) satisfies the following inequality:

$$\|\overline{x}_{ref\tau}\|_{L_\infty} \leq \|G(s)\|_{L_1} \|\lambda_{ref\tau}\|_{L_\infty} + \|H(s)C(s)k_g\|_{L_1} \|r\|_{L_\infty} + \|\overline{x}_{ref0}\|_{L_\infty} \tag{27}$$

First, assume that (24) does not hold. Consider that $\overline{x}_{ref}(t)$ is a continuous function and the following relationship holds $\|\overline{x}_{ref}(0)\|_\infty = \|\overline{x}(0)\|_\infty \leq \rho_0 < \rho_r$, then:

$$\begin{array}{l} \|\overline{x}_{ref}(t)\|_\infty < \rho_r, \forall t \in [0, \tau) \\ \|\overline{x}_{ref}(\tau)\|_\infty = \rho_r \end{array} \tag{28}$$

Therefore, the following equation is implied:

$$\|\overline{x}_{ref\tau}\|_{L_\infty} = \rho_r \tag{29}$$

Second, the following upper bound is obtained by recalling Assumption 2:

$$\|\lambda_{ref\tau}\|_{L_\infty} \leq L_{\rho_r}\rho_r + B_1 \tag{30}$$

Meanwhile, considering the definition of ρ_{in} in (18), the following expression can be obtained:

$$\|\overline{x}_{ref0}\|_{L_\infty} \leq \rho_{in} \tag{31}$$

Substituting inequalities (30) and (31) into (22), and combining with Lemma 2 yields:

$$\|\overline{x}_{ref\tau}\|_{L_\infty} \leq \|G(s)\|_{L_1}(L_{\rho_r}\rho_r + B_1) + \|H(s)C(s)k_g\|_{L_1}\|r\|_{L_\infty} + \rho_{in} \tag{32}$$

Based on the L1-norm condition (18), the following relationship is obtained:

$$\|G(s)\|_{L_1}(L_{\rho_r}\rho_r + B_1) + \|H(s)C(s)k_g\|_{L_1}\|r\|_{L_\infty} + \rho_{in} < \rho_r \tag{33}$$

Combining inequalities (32) and (33), $\|\overline{x}_{ref\tau}\|_{L_\infty} < \rho_r$ is obtained. Obviously, the conclusion is contrary to (29); therefore, (24) is proven.

Based on Lemma 2, the control law of the L1 reference system (21) can be rewritten as follows:

$$\|v_{ref\tau}\|_{L_\infty} \leq \left\|\frac{C(s)}{\omega}\right\|_{L_1}\left(|k_g|\|r\|_{L_\infty} + \|\lambda_{ref\tau}\|_{L_\infty}\right) \tag{34}$$

Substituting (30) into (34), it is obtained:

$$\|v_{ref}\|_{L_\infty} < \left\|\frac{C(s)}{\omega}\right\|_{L_1}\left(|k_g|\|r\|_{L_\infty} + L_{\rho_r}\rho_r + B_1\right) \tag{35}$$

Therefore, (25) is also proven. □

4.2. Analysis of Performance Boundaries

Based on (14) and (15), the prediction error equation can be obtained as follows:

$$\dot{\widetilde{\overline{x}}}(t) = \overline{A}\widetilde{\overline{x}}(t) + \overline{B}_h(\widetilde{\omega}(t)v(t) + \widetilde{\theta}(t)\|\overline{x}(t)\|_\infty + \widetilde{\sigma}(t)) \tag{36}$$

where $\widetilde{\overline{x}}(0) = 0, \widetilde{\omega}(t) = \hat{\omega}(t) - \omega(t), \widetilde{\theta}(t) = \hat{\theta}(t) - \theta(t)$, and $\widetilde{\sigma}(t) = \hat{\sigma}(t) - \sigma(t)$.

The following theorem verifies the performance boundaries of the closed-loop system (14):

Theorem 1. *For the closed-loop system (14), considering the L1 reference system (21) and the L1 adaptive controller consisting of (15)–(17) subject to the L1-norm condition (20), if* $\|\overline{x}(0)\|_\infty \leq \rho_0$, *then*

$$\|\widetilde{\overline{x}}\|_{L_\infty} \leq \alpha_0 \tag{37}$$

$$\|\overline{x}_{ref} - \overline{x}\|_{L_\infty} \leq \alpha_1 \tag{38}$$

$$\|v_{ref} - v\|_{L_\infty} \leq \alpha_2 \tag{39}$$

where $\alpha_0 = \sqrt{\frac{4\varpi_m}{\lambda_{\min}(P)\Gamma}}, \alpha_1 = \frac{\|C(s)\|_{L_1}}{1-\|C(s)\|_{L_1}L_{\rho_r}}\alpha_0 + \varepsilon$ *and* $\alpha_2 = \left\|\frac{C(s)}{\omega}\right\|_{L_1}L_{\rho_r}\alpha_1 + \left\|\frac{H_1(s)}{\omega}\right\|_{L_1}\alpha_0$, *in which* ε *is an arbitrarily small positive constant,* $H_1(s) = C(s)\frac{1}{c_0^T H(s)}c_0^T$, $H(s)$ *is introduced in the L1-norm condition (20) and* c_0 *is a vector that ensures the system* $H_1(s)$ *BIBO stable and proper,*

$$\varpi_m = \max_{\omega\in\Omega} tr(\omega^T\omega) + \theta_b^2 + \sigma_b^2 + \frac{\lambda_{\max}(P)}{\lambda_{\min}(Q)}(\theta_b d_\theta + \sigma_b d_\sigma).$$

Proof of Theorem 1. To prove (37), the Lyapunov function is chosen as follows:

$$V = \widetilde{\overline{x}}^T P \widetilde{\overline{x}} + \frac{1}{\Gamma}(tr(\widetilde{\omega}^T \widetilde{\omega}) + \widetilde{\theta}^T \widetilde{\theta} + \widetilde{\sigma}^T \widetilde{\sigma}) \tag{40}$$

$\dot{V}$ is derived as follows:

$$\dot{V} = \dot{\widetilde{\overline{x}}}^T P \widetilde{\overline{x}} + \widetilde{\overline{x}}^T P \dot{\widetilde{\overline{x}}} + \frac{2}{\Gamma}(tr(\widetilde{\omega}^T \dot{\widetilde{\omega}}) + \widetilde{\theta}^T \dot{\widetilde{\theta}} + \widetilde{\sigma}^T \dot{\widetilde{\sigma}}) \tag{41}$$

Substituting the adaptive laws in (16), (41) can be rewritten as follows:

$$\dot{V} \leq -\widetilde{\overline{x}}^T Q \widetilde{\overline{x}} + \frac{2}{\Gamma}(\left|tr(\widetilde{\omega}^T \dot{\omega})\right| + \left|\widetilde{\theta}^T \dot{\theta}\right| + \left|\widetilde{\sigma}^T \dot{\sigma}\right|) \tag{42}$$

Considering the boundaries of the unknown parameter θ and σ in Lemma 1, (41) is further simplified as follows:

$$\dot{V} \leq -\widetilde{\overline{x}}^T Q \widetilde{\overline{x}} + \frac{4}{\Gamma}(\theta_b d_\theta + \sigma_b d_\sigma) \tag{43}$$

Based on the boundaries of the unknown parameters ω, θ and σ, the following relationship can be derived:

$$tr(\widetilde{\omega}^T \widetilde{\omega}) + \widetilde{\theta}^T \widetilde{\theta} + \widetilde{\sigma}^T \widetilde{\sigma} \leq 4(\max_{\omega \in \Omega} tr(\omega^T \omega) + \theta_b^2 + \sigma_b^2) \tag{44}$$

According to the definition of V in (40), assume that the following inequality is true:

$$V > \frac{4}{\Gamma}\left[\max_{\omega \in \Omega} tr(\omega^T \omega) + \theta_b^2 + \sigma_b^2 + \frac{\lambda_{\max}(P)}{\lambda_{\min}(Q)}(\theta_b d_\theta + \sigma_b d_\sigma)\right] \tag{45}$$

where $\lambda_{\min}(Q)$ and $\lambda_{\max}(P)$ represent the minimum and maximum eigenvalues of matrices Q, P, respectively.

Based on (44) and (45), the following is obtained:

$$\widetilde{\overline{x}}^T P \widetilde{\overline{x}} = V - \frac{1}{\Gamma}(tr(\widetilde{\omega}^T \widetilde{\omega}) + \widetilde{\theta}^T \widetilde{\theta} + \widetilde{\sigma}^T \widetilde{\sigma}) > \frac{4\lambda_{\max}(P)}{\Gamma \lambda_{\min}(Q)}(\theta_b d_\theta + \sigma_b d_\sigma) \tag{46}$$

Therefore, the following inequality can hold:

$$\widetilde{\overline{x}}^T Q \widetilde{\overline{x}} \geq \frac{\lambda_{\min}(Q)}{\lambda_{\max}(P)} \widetilde{\overline{x}}^T P \widetilde{\overline{x}} > \frac{4}{\Gamma}(\theta_b d_\theta + \sigma_b d_\sigma) \tag{47}$$

Based on (43) and (47), $\dot{V}$ is derived as follows:

$$\dot{V} < 0 \tag{48}$$

According to (44) and (46), the following relation is valid:

$$V(t) \leq V(0) \leq \frac{4}{\Gamma}\left[\max_{\omega \in \Omega} tr(\omega^T \omega) + \theta_b^2 + \sigma_b^2\right] \tag{49}$$

It is obvious that (49) is contrary to the assumption in (45). Therefore, the following relationship is developed:

$$V \leq \frac{4}{\Gamma}\left[\max_{\omega \in \Omega} tr(\omega^T \omega) + \theta_b^2 + \sigma_b^2 + \frac{\lambda_{\max}(P)}{\lambda_{\min}(Q)}(\theta_b d_\theta + \sigma_b d_\sigma)\right] \tag{50}$$

Meanwhile, consider the following inequalities:

$$\lambda_{\min}(P)\|\widetilde{\overline{x}}\|^2 \leq \widetilde{\overline{x}}^T P\widetilde{\overline{x}} \leq V \tag{51}$$

Substituting (50) into (51), the following boundary of $\widetilde{\overline{x}}$ is obtained:

$$\|\widetilde{\overline{x}}\|_{L_\infty} \leq \sqrt{\frac{4\varpi_m}{\lambda_{\min}(P)\Gamma}} \tag{52}$$

Therefore, (37) is proven.

Based on (36), the L1 adaptive control law in (17) can be rewritten as follows:

$$v(s) = -C(s)(\omega v(s) + \chi_0(s) + \widetilde{\chi}(s) - k_g r(s)) \tag{53}$$

where χ_0 and $\widetilde{\chi}$ are defined as: $\chi_0(t) = \theta(t)\|\overline{x}(t)\|_\infty + \sigma(t)$ and $\widetilde{\chi}(t) = \widetilde{\omega}v(t) + \widetilde{\theta}(t)\|\overline{x}(t)\|_\infty + \widetilde{\sigma}(t)$.

Equation (53) is further simplified to obtain the following:

$$v(s) = \frac{-C(s)}{\omega}(\chi_0(s) + \widetilde{\chi}(s) - k_g r(s)) \tag{54}$$

Based on (18) and (54), the state equation in (14) is converted to frequency domain form as follows:

$$\overline{x}(s) = H(s)C(s)k_g r(s) - H(s)C(s)\widetilde{\chi}(s) + G(s)\chi_0(s) + (sI - \overline{A})^{-1}\overline{x}_0(s) \tag{55}$$

Considering the definitions of $\overline{x}_{ref0}$ in (22), $\widetilde{\chi}$ in (53) and $\widetilde{\overline{x}}$ in (36), it is determined that $\widetilde{\overline{x}}(s) = H(s)\widetilde{\chi}(s)$. Thus, the subtraction of (22) and (55) is equal to

$$\overline{x}_{ref}(s) - \overline{x}(s) = G(s)(\lambda_{ref}(s) - \chi_0(s)) + C(s)\widetilde{\overline{x}}(s) \tag{56}$$

Using the Lipschitz continuity [39] and the definition of L_{ρ_r} in (18), one obtains the following:

$$\left|\left|(\lambda_{ref} - \chi_0)_\tau\right|\right|_{L_\infty} \leq L_{\rho_r}\left|\left|(\overline{x}_{ref} - \overline{x})_\tau\right|\right|_{L_\infty} \tag{57}$$

Based on the application of Lemma 2 and (57), (56) can be rewritten as follows:

$$\left|\left|(\overline{x}_{ref} - \overline{x})_\tau\right|\right|_{L_\infty} \leq ||G(s)||_{L_1} L_{\rho_r}\left|\left|(\overline{x}_{ref} - \overline{x})_\tau\right|\right|_{L_\infty} + ||C(s)||_{L_1}\left|\left|\widetilde{\overline{x}}_\tau\right|\right|_{L_\infty} \tag{58}$$

Noting the boundary of $\widetilde{\overline{x}}$ in (37), (58) is organized as follows:

$$\|(\overline{x}_{ref} - \overline{x})_\tau\|_{L_\infty} \leq \frac{\|C(s)\|_{L_1}}{1 - \|G(s)\|_{L_1} L_{\rho_r}}\alpha_0 \tag{59}$$

Based on the definition of α_1 in (38), one can write the following:

$$\|(\overline{x}_{ref} - \overline{x})_\tau\|_{L_\infty} \leq \alpha_1 - \varepsilon < \alpha_1 \tag{60}$$

Therefore, (38) is proven.

Based on the reference control law v_{ref} in (21) and (54), the following equation is derived:

$$v_{ref}(s) - v(s) = -\frac{C(s)}{\omega}(\lambda_{ref}(s) - \chi_0(s) - \widetilde{\chi}(s)) \tag{61}$$

Let $H_1(s) = C(s)\frac{1}{c_0^T H(s)}c_0^T$ and c_0 is introduced to guarantee that $H_1(s)$ is a proper and stable system. Thus, the following relationship is obtained:

$$\frac{C(s)}{\omega}\widetilde{\chi}(s) = \frac{1}{\omega}H_1(s)\widetilde{\overline{x}}(s) \tag{62}$$

Based on the application of Lemma 2 and (62), (61) can be rewritten as follows:

$$\|(v_{ref} - v)_\tau\|_{L_\infty} \leq \left\|\frac{C(s)}{\omega}\right\|_{L_1} L_{\rho_r}\|(\overline{x}_{ref} - \overline{x})_\tau\|_{L_\infty} + \left\|\frac{H_1(s)}{\omega}\right\|_{L_1}\|\widetilde{\overline{x}}\|_{L_\infty} \tag{63}$$

Substituting (37) and (38) into (63), (39) is proven. □

Remark 7. *The upper boundary of (37) implies that an infinitesimal boundary α_0 can be obtained by increasing the adaptive gain Γ, and α_1, α_2 can also converge to infinitesimal according to (38) and (39). In practice, the adaptive gain Γ cannot be increased indefinitely due to robustness and hardware limitations, which is considered as a compromise.*

5. Simulation Results

To verify the performance of the proposed controller, a nonlinear system model is used for simulation, subject to input constraint, external disturbances, and the concurrency of actuator and sensor faults. Considering that the reference signal may be constant or time-varying, the reference inputs here are chosen as follows: $r(t) = 1$ and $r(t) = \sin(\frac{\pi}{3}t)$. In the process of converting the sensor faults to the pseudo-actuator faults, the selected parameters of the low-pass filter are $A_l = -4.499, B_l = 12$. The control input saturation of the system is set to $u_m = 5$ and $h^* = 15$. The nonlinear system is modeled as shown in (1), and the relevant parameters are set as follows:

$$A = \begin{bmatrix} -2.5 & 1.5 \\ -1 & -1.4 \end{bmatrix}, B = \begin{bmatrix} 0 \\ 1 \end{bmatrix}, C = \begin{bmatrix} 1 & 0 \end{bmatrix}, d(t) = \begin{bmatrix} \cos t \\ \sin t \end{bmatrix},$$

$$f(x,t) = (x_2 \cos x_1 + \cos x_2^2)\begin{bmatrix} 1 \\ 1 \end{bmatrix}.$$

Based on the meaning of the augmented matrices in (6) and (12), the coefficient matrices of system model (12) can be calculated as follows:

$$\overline{A} = \begin{bmatrix} -2.5 & 1.5 & 0 \\ -1 & -1.4 & 0 \\ 11.99 & 0 & -4.499 \end{bmatrix}, \overline{B}_h = \begin{bmatrix} 0 \\ 15 \\ 0 \end{bmatrix}, \overline{C} = \begin{bmatrix} 0 & 0 & 1 \end{bmatrix}.$$

The main parameters of the L1 adaptive controller are as follows:

$$P = \begin{bmatrix} 0.9501 & 0.3275 & 0.1837 \\ 0.3275 & 0.708 & 0.0467 \\ 0.1837 & 0.0467 & 0.1111 \end{bmatrix}, k_g = 0.0834, \Gamma = 10^5.$$

The low-pass filter $C(s)$ is set as follows:

$$C(s) = \frac{0.0005s + 1}{0.25s + 1}$$

The simulation experiments described in this section are carried out in the following four cases:

Case 1. No faults

The simulation results considering only control input constraint and external disturbances are presented in Figure 2, where both actuators and sensors are working properly.

The curves of the tracking performance when $r(t) = 1$ and $r(t) = \sin(\frac{\pi}{3}t)$ in Figure 2a,b show the reference input r, the system output y, and the deviation between them. As can be observed in Figure 2a,b, the system output y tracks the reference input r well with minimal deviation, regardless of whether the reference signal is constant or time-varying. The curve of the control input in Figure 2c shows that the control input signal can converge to the equilibrium position in a very short time, which has the advantage of good smoothness and convergence. Figure 2d illustrates the response curves of the original uncertainty, f, in the system model (1) and the lumped uncertainty, ζ_e, in the transformed system model (12). As can be observed from the response curves for the two uncertainties in Figure 2d, the lumped uncertainty is larger than the original uncertainty of the system due to input constraint and external disturbances, but both are convergent and smooth. The results in Figure 2 show that the system can well compensate for the influences of system uncertainties, control input constraint and external disturbances, and achieve fast and stable tracking.

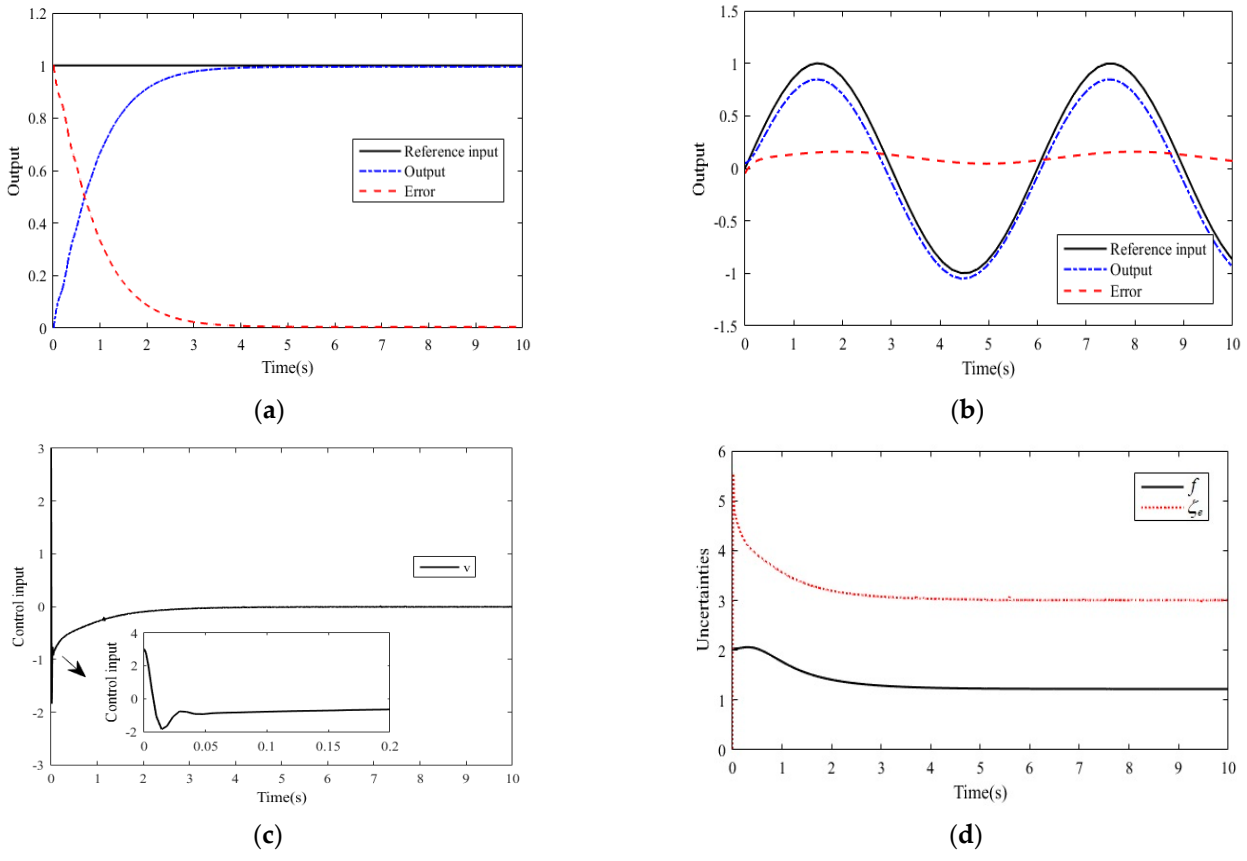

Figure 2. Simulation results when there is no fault. (**a**) Output curves of the system when $r(t) = 1$. (**b**) Output curves of the system when $r(t) = \sin(\frac{\pi}{3}t)$. (**c**) Curve of the control input when $r(t) = 1$. (**d**) Output curves of uncertainties f and ζ_e when $r(t) = 1$.

It should be noted that, due to the limitation of the length of this paper, Figure 2 does not show the output curves of the control input and uncertainties when $r(t) = \sin(\frac{\pi}{3}t)$. However, from the tracking curves in Figure 2b, it can be seen that the system achieves a good tracking when $r(t) = \sin(\frac{\pi}{3}t)$. It can also be deduced that the system's output curves of the control inputs and uncertainties are also convergent and smooth similar to those at $r(t) = 1$. This is true for all of the simulation results shown in Figures 3–7. On the basis of considering control input constraint and external disturbances, cases 2–4 are designed to demonstrate the fault tolerance of the system to both actuator and sensor faults, which include sensor faults, actuator faults, and simultaneous actuator and sensor faults, regardless of whether faults are constant or time-varying. Meanwhile, comparative simulation experiments of MRAC under the same parameter conditions are implemented.

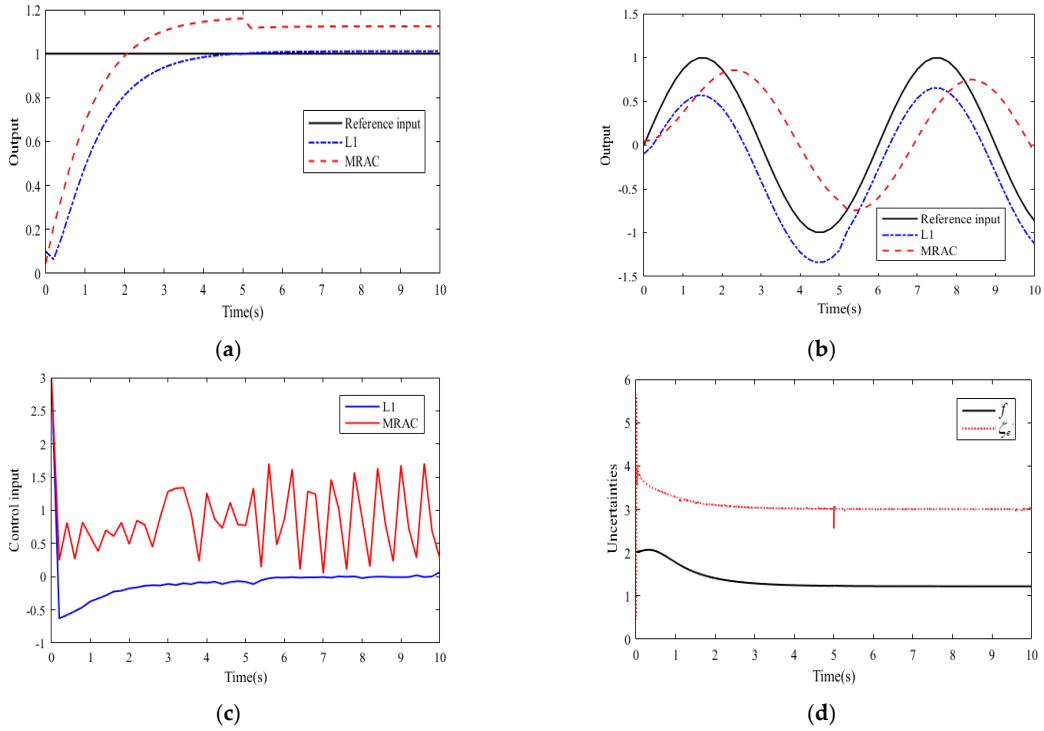

Figure 3. Simulation results when sensors have constant faults. (**a**) Output curves of the system when $r(t) = 1$. (**b**) Output curves of the system when $r(t) = \sin(\frac{\pi}{3}t)$. (**c**) Curves of the control input when $r(t) = 1$. (**d**) Output curves of uncertainties f and ζ_e when $r(t) = 1$.

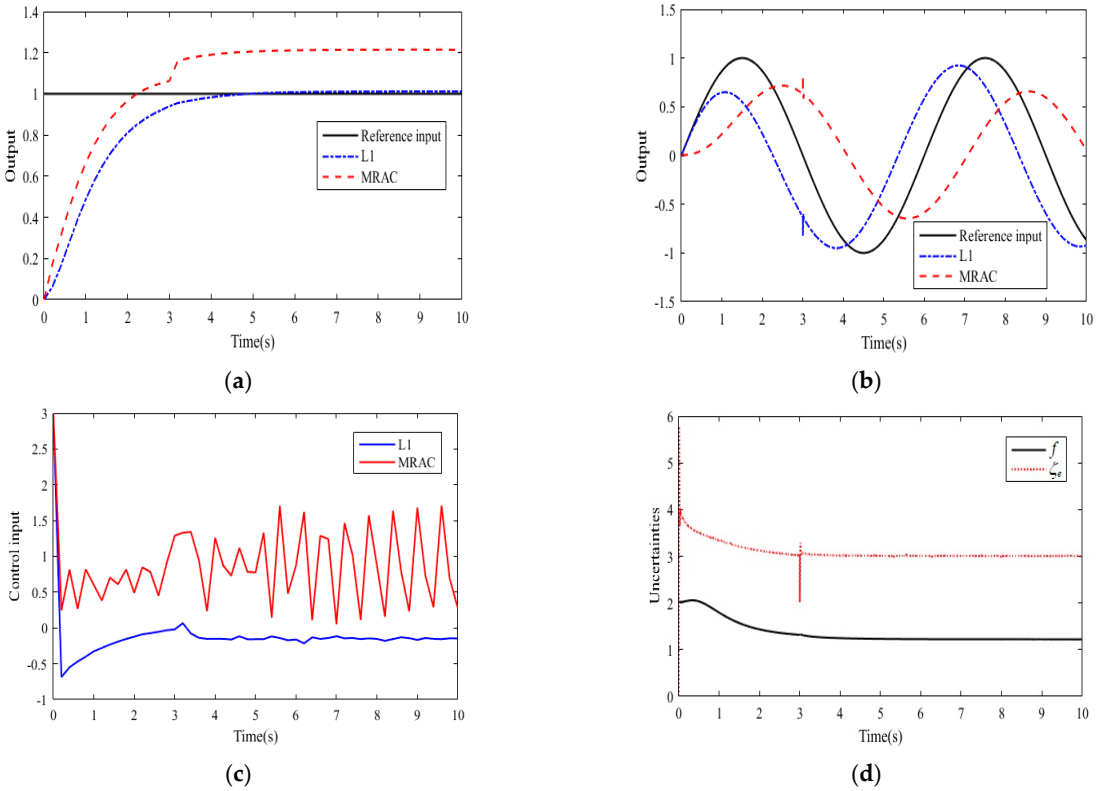

Figure 4. Simulation results when sensors have time-vary faults and constant faults. (**a**) Output curves of the system when $r(t) = 1$. (**b**) Output curves of the system when $r(t) = \sin(\frac{\pi}{3}t)$. (**c**) Curves of the control input when $r(t) = 1$. (**d**) Output curves of uncertainties f and ζ_e when $r(t) = 1$.

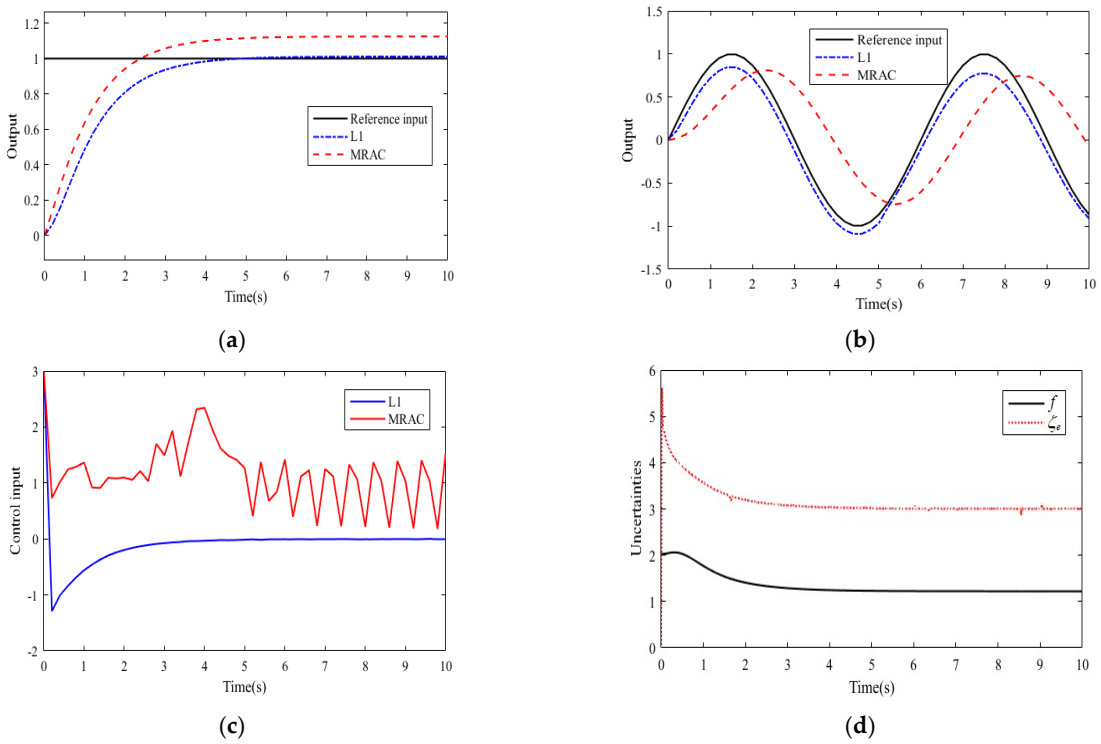

Figure 5. Simulation results when actuators have multiplicative faults. (**a**) Output curves of the system when $r(t) = 1$. (**b**) Output curves of the system when $r(t) = \sin(\frac{\pi}{3}t)$. (**c**) Curves of the control input when $r(t) = 1$. (**d**) Output curves of uncertainties f and ζ_e when $r(t) = 1$.

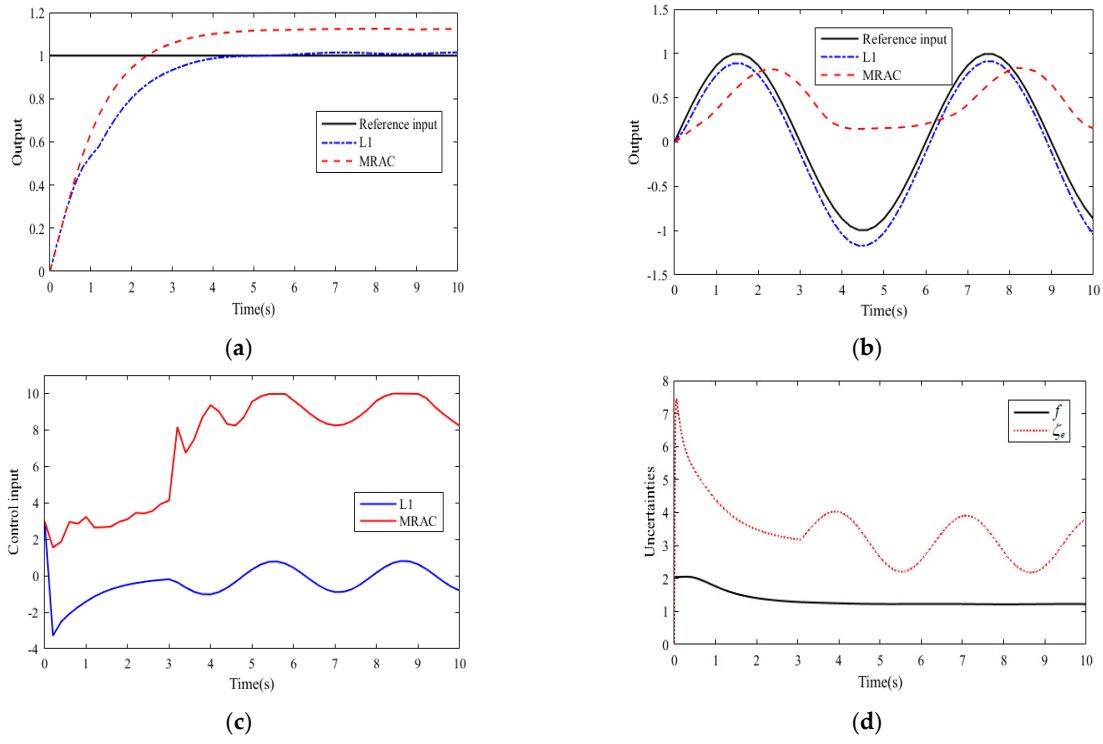

Figure 6. Simulation results when actuators have multiplicative faults and additive faults. (**a**) Output curves of the system when $r(t) = 1$. (**b**) Output curves of the system when $r(t) = \sin(\frac{\pi}{3}t)$. (**c**) Curves of the control input when $r(t) = 1$. (**d**) Output curves of uncertainties f and ζ_e when $r(t) = 1$.

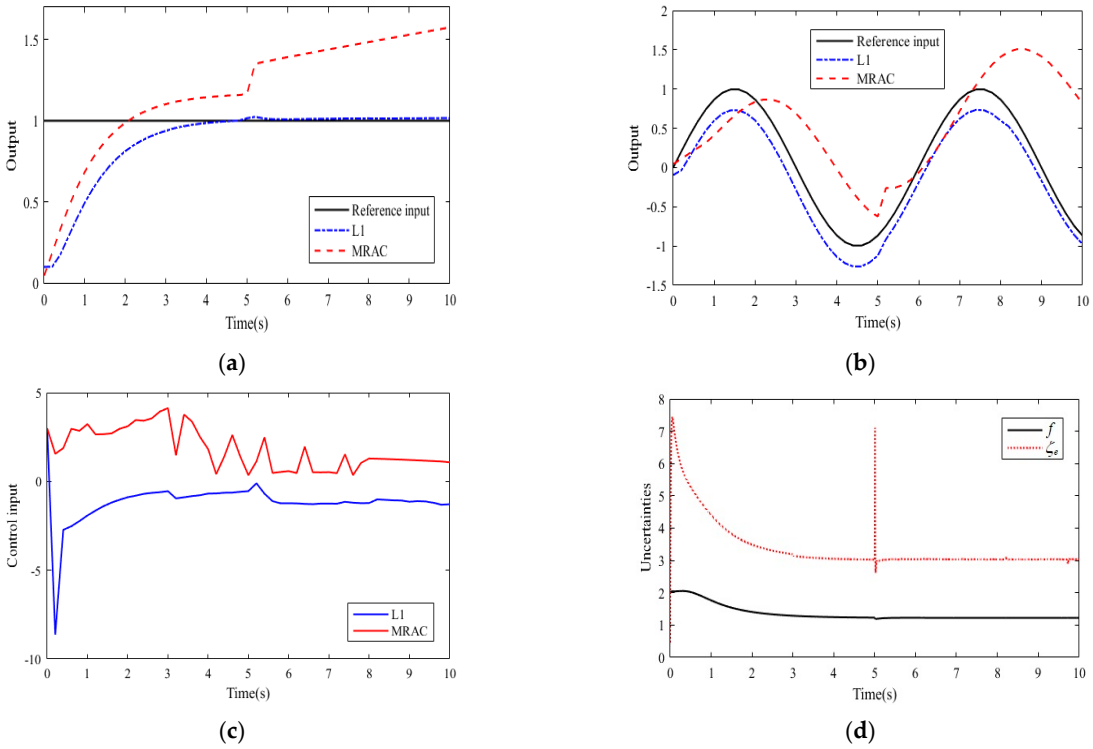

Figure 7. Simulation results when actuator faults and sensor faults occur simultaneously. (**a**) Output curves of the system when $r(t) = 1$. (**b**) Output curves of the system when $r(t) = \sin(\frac{\pi}{3}t)$. (**c**) Curves of the control input when $r(t) = 1$. (**d**) Output curves of uncertainties f and ζ_e when $r(t) = 1$.

Case 2. Sensor faults (constant faults and time-varying faults)

The following constant sensor faults are considered:

$$Gf_s = \begin{cases} \begin{bmatrix} 0.1 \\ 0.1 \end{bmatrix}, 0 \leq t < 5 \\ \begin{bmatrix} 0 \\ 0 \end{bmatrix}, t \geq 5 \end{cases}$$

This fault model indicates that the system suffers a constant bias sensor fault with a magnitude of 0.1 when $0 \leq t < 5$, and the sensors return to normal when $t \geq 5$. The simulation results of the L1 adaptive controller and MRAC are compared in Figure 3.

The simulation results when constant bias sensor faults occur in the system are shown in Figure 3. From the response curves in Figure 3a,b, it can be seen that the comparative MRAC responds faster than the L1 adaptive controller; however, the MRAC scheme has a larger tracking error with either constant or time-varying reference signals. The L1 adaptive controller possesses a lower overshoot and a smaller steady error. From the simulation results in Figure 3c, it can be seen that the control output of MRAC fluctuates more in order to compensate for the effects of sensor faults, input constraint and external disturbances, while the control output curve of the L1 adaptive controller fluctuates slightly around the equilibrium position, except for a very short period of time at the beginning of the simulation. As can be seen from the output curves of the uncertainties demonstrated in Figure 3d, there is a transient oscillation in the estimate of the lumped uncertainty when sensor faults occur at $t = 0$ as well as when sensors return to normal operation at $t = 5$; at other moments, the lumped uncertainty maintains a consistent and bounded estimate. The L1 adaptive controller shows good stability and fault tolerance performance when the sensors have constant bias faults.

The following time-varying and constant sensor faults are considered:

$$Gf_s = \begin{cases} \begin{bmatrix} 3\sin t \\ 3\sin t \end{bmatrix}, 0 \le t < 3 \\ \begin{bmatrix} 0.2 \\ 0.2 \end{bmatrix}, t \ge 3 \end{cases}$$

This fault shows that the system has a time-varying sensor fault of sinusoidal form when $0 \le t < 3$, and the sensors have constant bias faults with a magnitude of 0.2 when $t \ge 3$. The simulation results of the L1 adaptive controller and MRAC are compared in Figure 4.

The simulation results considering both time-varying and constant sensor faults are shown in Figure 4. From Figure 4a,b, it can be observed that the L1 adaptive controller has superior tracking performance compared with MRAC. This can be clearly seen from the steady-state error, which reaches 20% for MRAC in Figure 4a and is even higher in Figure 4b, while the L1 adaptive controller is almost zero. A comparison of the response curves in both Figure 3c,d and Figure 4c,d shows that the presentation is similar except that the control signals and uncertainty estimates are somewhat different at the moment of fault occurrence. This indicates that the L1 adaptive controller outputs smoother and faster convergence with more stable performance. Combined with Figures 3 and 4, it can be seen that the L1 adaptive controller can compensate well for the influences of sensor faults, input constraint and external disturbances; moreover, it can realize accurate and stable tracking of a given constant or time-varying input signal.

Case 3. Actuator faults (multiplicative faults and additive faults)

The following multiplicative actuator faults are considered:

$$\omega = \begin{cases} \begin{bmatrix} 0.5 & 0 \\ 0 & 0.5 \end{bmatrix}, 0 \le t < 5 \\ \begin{bmatrix} 1 & 0 \\ 0 & 1 \end{bmatrix}, t \ge 5 \end{cases}$$

This fault model shows that actuators have constant multiplicative faults with $\omega = 0.5$ when $0 \le t < 5$, which implies that the actuators lose half of their effectiveness. Furthermore, the actuator faults are eliminated when $t \ge 5$. The simulation results of the L1 adaptive controller and MRAC are compared in Figure 5.

From Figure 5a,b, it can be seen that the tracking error of the L1 adaptive controller is smaller than that of MRAC, while the overshoot is also smaller. Moreover, Figure 5c shows that the MRAC has large fluctuations in the control inputs in order to compensate for the effect of actuator faults, whereas the L1 adaptive controller has very small and smoother fluctuations and converges more quickly. Figure 5d clearly demonstrates that the L1 adaptive controller also guarantees a smooth and bounded lumped uncertainty estimation. Figure 5 shows that the L1 adaptive controller designed in this paper has a better control performance under the action of constant multiplicative actuator faults, providing the advantages of strong tracking performance, a smooth and bounded control input signal, and uncertainty estimation.

The following multiplicative and additive actuator fault model is also considered:

$$\omega = \begin{cases} \begin{bmatrix} 0.2 & 0 \\ 0 & 0.2 \end{bmatrix}, 0 \le t < 3 \\ \begin{bmatrix} 0.1 & 0 \\ 0 & 0.1 \end{bmatrix}, t \ge 3 \end{cases}, \overline{u} = \begin{cases} O_{2\times 2}, 0 \le t < 3 \\ \begin{bmatrix} 5\sin 2t & 0 \\ 0 & 5\sin 2t \end{bmatrix}, t \ge 3 \end{cases}$$

This fault model shows that the actuators have constant multiplicative faults with $\omega = 0.2$ when $0 \le t < 3$, which indicates that actuators lose 80% of their effectiveness. The actuators endure constant multiplicative faults and time-varying additive faults when

$t \geq 3$. The simulation results of the L1 adaptive controller and MRAC are compared in Figure 6.

The response curves of the system with multiplicative and additive actuator faults are shown in Figure 6. From Figure 6c, it can be seen that when multiplicative and additive actuator faults occur at the same time, the L1 adaptive controller outputs smoother control signals to compensate for these faults. It can clearly be observed that the tracking error of MRAC reaches more than 10% in Figure 6a and even larger in Figure 6b, while the L1 adaptive controller still converges to zero as in the case of a single multiplicative fault. Figure 6d illustrates that when additive actuator faults are added at $t = 3$, the estimate of the lumped uncertainty ζ_e presents a larger fluctuation compared with the previous moments when only a single multiplicative fault is present, but still maintains a bounded and smooth estimation. A look at Figures 5 and 6 reveals that the L1 adaptive controller has better tracking performance, stronger stability, and fault tolerance than MRAC.

Case 4. Actuator faults and sensor faults (constant faults and time-varying faults)

The following multiple faults are considered:
Actuator faults:

$$\omega = \begin{cases} \begin{bmatrix} 0.2 & 0 \\ 0 & 0.2 \end{bmatrix}, 0 \leq t < 3 \\ \begin{bmatrix} 0.1t & 0 \\ 0 & 0.1t \end{bmatrix}, 3 \leq t < 8 \\ \begin{bmatrix} 0.8 & 0 \\ 0 & 0.8 \end{bmatrix}, t \geq 8 \end{cases}, \overline{u} = \begin{cases} O_{2\times 2}, 0 \leq t < 3 \\ \begin{bmatrix} 0.2 & 0 \\ 0 & 0.2 \end{bmatrix}, 3 \leq t < 8 \\ O_{2\times 2}, t \geq 8 \end{cases}$$

Sensor faults:

$$Gf_s = \begin{cases} \begin{bmatrix} 0.1 & 0 \\ 0 & 0.1 \end{bmatrix}, 0 \leq t < 5 \\ \begin{bmatrix} 0.2t & 0 \\ 0 & 0.2t \end{bmatrix}, t \geq 5 \end{cases}$$

This fault model shows that the actuators have constant multiplicative faults with $\omega = 0.2$ when $0 \leq t < 3$, which indicates that actuators have only 20% of control effectiveness. The actuators have time-varying multiplicative faults and constant additive faults when $3 \leq t < 8$, and there are only constant multiplicative faults in the system when $t \geq 8$. Meanwhile, the sensors have constant bias faults with a magnitude of 0.1 when $0 \leq t < 5$, and have time-varying faults when $t \geq 5$. The simulation results of the L1 adaptive controller and MRAC are compared in Figure 7.

From Figure 7a,b, it can be seen that the output signal of MRAC cannot track the reference input r well and the tracking error keeps increasing from $t \geq 5$, due to the simultaneous effect of actuator and sensor faults. On the other hand, the output signals of the L1 adaptive controller maintain smooth and stable responses, except for slight fluctuations at the moment of faults occurrence. The control input curve of the L1 adaptive controller in Figure 7c shows that at the moments when the faults change, ($t = 3, t = 5$ and $t = 8$), the control input signal oscillates slightly in order to counteract the performance degradation caused by the faults, but quickly returns to the equilibrium position. The control input signal is stable and converges fast. Meanwhile, the control signal of MRAC oscillates for a period of time before stabilizing; the same is valid for the lumped uncertainty estimation curve illustrated in Figure 7d. Synthesizing the response curves in Figures 2–7, it can be concluded that the L1 adaptive controller exhibits excellent tracking performance, good stability, and fault tolerance in all four simulation scenarios.

6. Conclusions

In this paper, an L1 adaptive fault-tolerant controller against multiple faults, input constraint, and external disturbances was designed. Sensor faults and input constraint are transformed and reorganized through state expansion and nonlinear function approxima-

tion. Combined with actuator faults, external disturbances, and approximation errors, an uncertain nonlinear system with unknown parameters and lumped uncertainties was developed. Moreover, the design of the L1 adaptive fault-tolerant controller compensates for the effects of uncertainties. With the integrated effect of the state predictor, adaptive laws, and control law components, the L1 adaptive controller achieves concise and effective control without additional fault observers or estimators. The comparative simulation results demonstrate that the designed controller has good stability, fault tolerance, and tracking performance. The performance of the proposed controller will be further implemented and validated in the future using nonlinear systems such as unmanned aerial vehicles and unmanned surface vehicles. Meanwhile, fault-tolerant control for other types of sensor faults, such as stuck faults and loss of effectiveness faults, is another future research direction.

Author Contributions: Conceptualization, Y.Z. and H.G.; methodology, H.L.; software, Y.Z.; validation, H.L. and Y.Z.; formal analysis, Y.Z.; writing—original draft preparation, H.G.; writing—review and editing, Y.Z. All authors have read and agreed to the published version of the manuscript.

Funding: This work was supported by the Key Fields Special Project of Guangdong Provincial Colleges and Universities under grant 2021ZDZX1082.

Data Availability Statement: The data are contained within the article.

Conflicts of Interest: The authors declare no conflicts of interest.

References

1. Chen, L.; Alwi, H.; Edwards, C.; Sato, M. Flight evaluation of an LPV sliding mode observer for sensor FTC. *IEEE Trans. Control Syst. Technol.* **2022**, *30*, 1319–1327. [CrossRef]
2. Xiao, S.Y.; Dong, J.X. Robust adaptive fault-tolerant tracking control for uncertain linear systems with actuator failures based on the closed-loop reference model. *IEEE Trans. Syst. Man Cybern. Syst.* **2020**, *50*, 3448–3455. [CrossRef]
3. Gao, Z.; Chen, Y.D.; Li, W.Q.; Song, Y.D. Robust adaptive fault-tolerant proportional-derivative tracking control for six-degrees of freedom unmanned aerial vehicles. *Int. J. Robust Nonlinear Control* **2022**, *32*, 9761–9775. [CrossRef]
4. Cao, L.; Li, H.Y.; Dong, G.W.; Lu, R.Q. Event-triggered control for multiagent systems with sensor faults and input saturation. *IEEE Trans. Syst. Man Cybern. Syst.* **2021**, *51*, 3855–3866. [CrossRef]
5. Ding, R.Q.; Cheng, M.; Zheng, S.; Xu, B. Sensor-fault-tolerant operation for the independent metering control system. *IEEE-ASME Trans. Mechatron.* **2021**, *26*, 2558–2569. [CrossRef]
6. Wang, B.; Shen, Y.Y.; Zhang, Y.M. Active fault tolerant control for a quadrotor helicopter against actuator faults and model uncertainties. *Aerosp. Sci. Technol.* **2020**, *99*, 105745. [CrossRef]
7. Kazemi, H.; Yazdizadeh, A. Optimal state estimation and fault diagnosis for a class of nonlinear systems. *IEEE/CAA J. Autom.* **2020**, *7*, 517–526. [CrossRef]
8. Wang, R.J.; Zhao, C.J.; Bai, Y.; Du, W.H.; Wang, J.Y. An actuator fault detection and reconstruction scheme for hex-rotor unmanned aerial vehicle. *IEEE Access* **2019**, *7*, 93937–93951. [CrossRef]
9. Huang, C.; Huang, H.L.; Naghdy, F.; Du, H.P.; Ma, D.Z. Actuator fault tolerant control for steer-by-wire systems. *Int. J. Control* **2021**, *94*, 3123–3134. [CrossRef]
10. Kang, Y.F.; Yao, L.; Wang, H. Fault isolation and fault-tolerant control for Takagi-Sugeno fuzzy time-varying delay stochastic distribution systems. *IEEE Trans. Fuzzy Syst.* **2022**, *30*, 1185–1195. [CrossRef]
11. Xu, D.Z.; Zhu, F.L.; Zhou, Z.P.; Yan, X.G. Distributed fault detection and estimation in cyber–physical systems subject to actuator faults. *ISA Trans.* **2020**, *104*, 162–174. [CrossRef]
12. Liu, C.; Jiang, B.; Patton, R.J.; Zhang, K. Hierarchical structure-based adaptive fault-tolerant consensus control for multiple 3-DOF laboratory helicopters. *Int. J. Adapt. Control* **2020**, *34*, 992–1012. [CrossRef]
13. Liu, C.; Zhao, X.; Wang, X.F.; Ren, X.Q. Adaptive fault identification and reconfigurable fault-tolerant control for unmanned surface vehicle with actuator magnitude and rate faults. *Int. J. Robust Nonlinear Control* **2023**, *33*, 5463–5483. [CrossRef]
14. Zhong, Y.J.; Zhang, Y.M.; Ge, S.Z.S.; He, X. Robust distributed sensor fault detection and diagnosis within formation control of multiagent systems. *IEEE Trans. Aerosp. Electron. Syst.* **2023**, *59*, 1340–1353. [CrossRef]
15. Lyu, P.; Liu, S.C.; Lai, J.Z.; Liu, J.Y. An analytical fault diagnosis method for yaw estimation of quadrotors. *Control Eng. Pract.* **2019**, *86*, 118–128. [CrossRef]
16. Lu, P.; Kampen, E.J.V.; Visser, C.D.; Chu, Q.P. Air data sensor fault detection and diagnosis in the presence of atmospheric turbulence: Theory and experimental validation with real flight data. *IEEE Trans. Control Syst. Technol.* **2021**, *29*, 2255–2263. [CrossRef]
17. Wang, H.; Yao, L.N. Sensor fault diagnosis and fault-tolerant control for stochastic distribution time-delayed control systems. *Int. J. Adapt. Control* **2019**, *33*, 1395–1406. [CrossRef]

18. Chen, F.Y.; Gong, J.X.; Li, Y.Q. Adaptive diagnosis and compensation for hypersonic flight vehicle with multisensor faults. *Int. J. Robust Nonlinear Control* **2019**, *29*, 6145–6163. [CrossRef]
19. Ma, X.J.; Liu, S.Q.; Cheng, H.H. Civil aircraft fault tolerant attitude tracking based on extended state observers and nonlinear dynamic inversion. *J. Syst. Eng. Electron.* **2022**, *33*, 180–187. [CrossRef]
20. Wang, J.Q.; Fang, F.; Yi, X.J.; Liu, Y.J. Dynamic event-triggered fault estimation and sliding mode fault-tolerant control for networked control systems with sensor faults. *Appl. Math. Comput.* **2021**, *389*, 125558. [CrossRef]
21. Ding, J.Y.; Liu, Y.; Yu, J.Y.; Yang, X.B. Dissipativity-based integrated fault estimation and fault tolerant control for IT2 polynomial fuzzy systems with sensor and actuator faults. *IEEE Trans. Fuzzy Syst.* **2023**, *31*, 2956–2965. [CrossRef]
22. Zhu, L.; Li, X.F.; Huang, D.Q.; Dong, H.R.; Cai, L.C. Distributed cooperative fault-tolerant control of high-speed trains with input saturation and actuator faults. *IEEE Trans. Intell. Veh.* **2023**, *8*, 1241–1251. [CrossRef]
23. Yang, C.G.; Huang, D.Y.; He, W.; Cheng, L. Neural control of robot manipulators with trajectory tracking constraints and input saturation. *IEEE Trans. Neural Netw. Learn.* **2021**, *32*, 4231–4242. [CrossRef] [PubMed]
24. Do, V.T.; Lee, S.G. Neural integral backstepping hierarchical sliding mode control for a ridable ballbot under uncertainties and input saturation. *IEEE Trans. Syst. Man Cybern. Syst.* **2021**, *51*, 7214–7227. [CrossRef]
25. Zhang, Y.Q.; Liu, Y.J.; Liu, L. Minimal learning parameters-based adaptive neural control for vehicle active suspensions with input saturation. *Neurocomputing* **2020**, *396*, 153–161. [CrossRef]
26. Wei, Y.L.; Sheng, L.; Gao, M.; Ma, Y.H. Anti-saturation fault-tolerant control for Markov jump nonlinear systems with unknown control coefficients and unmodeled dynamics. *Nonlinear Anal. Hybrid* **2023**, *50*, 101384. [CrossRef]
27. Liang, H.J.; Liu, G.L.; Huang, T.W.; Lam, H.K.; Wang, B.H. Cooperative fault-tolerant control for networks of stochastic nonlinear systems with nondifferential saturation nonlinearity. *IEEE Trans. Syst. Man Cybern. Syst.* **2022**, *52*, 1362–1372. [CrossRef]
28. Hu, Q.L.; Shao, X.D.; Guo, L. Adaptive fault-tolerant attitude tracking control of spacecraft with prescribed performance. *IEEE-ASME Trans. Mechatron.* **2018**, *23*, 331–341. [CrossRef]
29. Yan, X.H.; Chen, M.; Feng, G.; Wu, Q.X.; Shao, S.Y. Fuzzy robust constrained control for nonlinear systems with input saturation and external disturbances. *IEEE Trans. Fuzzy Syst.* **2021**, *29*, 345–356. [CrossRef]
30. Yu, Z.Q.; Qu, Y.H.; Zhang, Y.M. Distributed fault-tolerant cooperative control for multi-UAVs under actuator fault and input saturation. *IEEE Trans. Control Syst. Technol.* **2019**, *27*, 2417–2429. [CrossRef]
31. Yu, Z.Q.; Zhang, Y.M.; Jiang, B.; Fu, J.; Jin, Y.; Chai, T.Y. Composite adaptive disturbance observer-based decentralized fractional-order fault-tolerant control of networked UAVs. *IEEE Trans. Syst. Man Cybern. Syst.* **2022**, *52*, 799–813. [CrossRef]
32. Lee, D.; Leeghim, H. Reaction wheel fault-tolerant finite-time control for spacecraft attitude tracking without unwinding. *Int. J. Robust Nonlinear Control* **2020**, *30*, 3672–3691. [CrossRef]
33. Gao, J.W.; Fu, Z.M.; Zhang, S. Adaptive fixed-time attitude tracking control for rigid spacecraft with actuator faults. *IEEE Trans. Ind. Electron.* **2019**, *66*, 7141–7149. [CrossRef]
34. Yang, P.; Liu, P.; Wen, C.W.; Geng, H.L. Fault-tolerant control for a class of n-order systems based on fast terminal sliding mode and extended state observer. *Meas. Control-UK* **2021**, *54*, 1234–1244. [CrossRef]
35. Bayless, J.A.; Voglewede, P.A. Joystick steering in recreational boats using L1 adaptive control. *J. Dyn. Syst. Meas. Control* **2020**, *142*, 064501. [CrossRef]
36. Alyazidi, N.M.; Mahmoud, M.S. L1 adaptive networked controller for islanded distributed generation systems in a microgrid. *Int. J. Syst. Sci.* **2018**, *49*, 2507–2524. [CrossRef]
37. Park, H.S.; Kim, Y.D. Adaptive fault tolerant flight control for input redundant systems using a nonlinear reference model. *IEEE Trans. Aerosp. Electron. Syst.* **2021**, *57*, 3337–3356. [CrossRef]
38. Cao, C.Y.; Hovakimyan, N. L1 adaptive controller for a class of systems with unknown nonlinearities: Part I. In Proceedings of the 2008 ACC, Seattle, WA, USA, 11–13 June 2008; pp. 4093–4098. [CrossRef]
39. Cao, C.Y.; Hovakimyan, N. Novel L1 neural network adaptive control architecture with guaranteed transient performance. *IEEE Trans. Neural Netw.* **2007**, *18*, 1160–1171. [CrossRef]
40. Pomet, J.B.; Praly, L. Adaptive Nonlinear Regulation: Estimation from the Lyapunov Equation. *IEEE Trans. Autom. Control.* **1992**, *37*, 729–740. [CrossRef]

Disclaimer/Publisher's Note: The statements, opinions and data contained in all publications are solely those of the individual author(s) and contributor(s) and not of MDPI and/or the editor(s). MDPI and/or the editor(s) disclaim responsibility for any injury to people or property resulting from any ideas, methods, instructions or products referred to in the content.